A New Possibility of Generalized Two-Dimensional Correlation Spectroscopy: Hybrid Two-Dimensional Correlation Spectroscopy

Yuqing Wu,[†,‡] Jian-Hui Jiang,[†,§] and Yukihiro Ozaki*[,†]

Department of Chemistry, School of Science, Kwansei-Gakuin University, Sanda, Hyogo 669-1337, Japan, Key Laboratory for Supramolecular Structure and Materials of the Ministry of Education, Jilin University, Changchun 130023, P. R. China, and College of Chemistry and Chemical Engineering, Hunan University, Changsha 410082, P. R. China

Received: June 5, 2001; In Final Form: November 30, 2001

In this paper, we propose a new possibility for generalized two-dimensional (2D) correlation spectroscopy, hybrid 2D correlation spectroscopy. Three types of hybrid 2D correlation spectroscopies are possible. In the first type, 2D correlation spectra are calculated by using two spectral data for the same sample obtained under two kinds of perturbations. In the second type, 2D correlation spectra are constructed by using spectral variations measured under conjunct or related perturbations. The third type treats 2D correlation spectra generated by using two independent spectral data obtained under the same perturbation but different conditions. In all the cases hybrid 2D correlation spectroscopy allows one to discuss directly the correlation between two independent spectral data sets and, therefore, extract additional information such as that about the comparison of effects of two different perturbations and the comparison of two different systems. In this paper we describe the principle of hybrid 2D correlation spectroscopy and demonstrate one example of type III. Hybrid 2D correlation spectroscopy has been applied to time-dependent infrared (IR) spectra of two kinds of reactions of the hydrogenation of nitrobenzene. One is complete reaction of nitrobenzene, and the other is its catalyst-modified reaction. The sample−sample hybrid 2D correlation spectra reveal clearly the concentration dynamics of the intermediate in the catalyst-modified reaction, and the wavenumber−wavenumber hybrid 2D correlation spectra provide unambiguous band assignments of the intermediate and the product in the IR spectra of the reaction mixture in the 1510−1470 cm^{-1} region.

Introduction

Two-dimensional (2D) correlation spectroscopy has recently been a subject of keen interest from the points of both basic science and a variety of applications.[1−11] 2D correlation spectroscopy simplifies complex spectra consisting of many overlapped peaks and enhances spectral resolution by spreading peaks along the second dimension, enabling one to extract information that cannot be obtained straightforwardly from one-dimensional spectra.[1−11] The introduction of generalized 2D correlation spectroscopy in 1993 has extended markedly the potential of 2D correlation spectroscopy.[2] In generalized 2D correlation spectroscopy any kind of perturbation can be used and any kind of spectral data can be applied. The application to heterospectral analysis is also quite straightforward.[12−14]

More recently, there was another important progress in 2D correlation spectroscopy. Šašić et al. have proposed a new kind of 2D correlation spectroscopy.[15−17] It is called sample−sample correlation spectroscopy. In sample−sample correlation spectroscopy, 2D correlation maps having sample axes are generated instead of creating 2D maps with variable (wavelength or wavenumber) axes.[15] In the usual 2D (variable−variable) correlation spectroscopy, the correlations between bands are discussed while, in sample−sample correlation spectroscopy, concentration dynamics are investigated. Thus, variable−variable correlation spectroscopy and sample−sample correlation spectroscopy are totally complementary.

Šašić and Ozaki[18] have proposed yet another type of 2D correlation spectroscopy, statistical 2D correlation spectroscopy. This idea came from the 2D correlation approach by Barton et al.[19] Šašić and Ozaki[18] have presented several improvements concerning the objects and targets of correlation analysis as well as a relatively simple linear algebra presentation that the methodology uses.

However, for all the 2D correlation analyses until now, synchronous and asynchronous spectra have been constructed from a series of spectra obtained under one particular perturbation and for one particular system. There may be a few questions. Is it possible to construct 2D correlation spectra between two series of spectra measured under two different kinds of perturbations such as temperature and pressure? Can we generate 2D correlation spectra from two different but related systems such as the same reaction by different catalysts? Such kinds of questions may result in new breakthroughs in 2D correlation spectroscopy.

In general, a spectral intensity is represented as $\varphi(\nu, T)$, where ν and T indicate frequency (wavenumber or wavelength) and any kind of reasonable physical variable, such as temperature, concentration, pressure, pH, etc., respectively. It may also be possible to treat a spectral intensity with three independent variables as $\varphi(\nu, t, T)$. Three variables represent frequency and two kinds of physical variables. Let us consider an example of

* To whom all correspondence should be sent. Mailing address: Department of Chemistry, School of Science, Kwansei-Gakuin University, Gakuen, Sanda, Hyogo 669-1337, Japan. Fax: +81-795-65-9077. E-mail: ozaki@kwansei.ac.jp.

† Kwansei-Gakuin University.

‡ Jilin University.

§ Hunan University.

10.1021/jp012140g CCC: $22.00
Published on Web 02/16/2002

a spectral intensity $\varphi(\upsilon, t, T)$, taking three independent variables as wavenumber (υ), time (t), and temperature (T). One can obtain wavenumber−wavenumber 2D synchronous $\Phi(\upsilon_1, \upsilon_2)$ and asynchronous $\Psi(\upsilon_1, \upsilon_2)$ correlation spectra using time-dependent spectra while keeping T constant. One can also construct 2D correlation spectra using the dependence on T while keeping t constant. These are just the cases that we have been using so far.[1−20]

However, in some cases spectral changes may be obtained as functions of two physical variables.[20] For example, time and temperature may vary at the same time. These variables are usually physically coupled perturbation variables. In other words, the spectral intensity variations are obtained as functions of the physically coupled perturbations. It may be interesting to analyze spectral variations induced by conjugated changes by use of 2D correlation spectroscopy. Moreover, for some systems, two independent physical variables can induce analogous or related structural changes. For example, in some protein solutions, both temperature and pressure changes can cause similar protein aggregation or secondary structural modifications.[21,22] It would also be interesting to explore coeffects of different physical variables on one system.

When one investigates spectral changes caused by two physical variables, two series of 2D correlation spectra are usually calculated using the dependence of spectral intensity changes on a single perturbation while keeping another constant.[20] Then, one can compare the two independent 2D correlation analyses to extract additional information concerning the conjugated effects. However, correlation between two independent series of spectra of the same sample obtained on the basis of two kinds of perturbations or correlation between two systems may be explored directly also by one 2D correlation map.

The purpose of this study is to propose a new extension of generalized 2D correlation spectroscopy; we name it hybrid 2D correlation spectroscopy. By use of this method, one can explore directly the correlations between two systems or spectral data sets measured under two different perturbations. In other words, hybrid 2D correlation spectroscopy involves the analysis of correlation between two sets of spectra, which is a further development of the so-called hetero 2D correlation spectroscopy.[1−3,5,23] By analogy to the existing 2D correlation spectroscopy, hybrid 2D correlation spectroscopy also involves variable−variable and sample−sample correlation spectroscopy.

In this paper, we describe the theoretical explanation of the hybrid 2D correlation analysis first and then demonstrate its application to time-dependent infrared (IR) spectra of two kinds of reactions of the catalytic hydrogenation of nitrobenzene.[24] Figure 1 shows the two kinds of reactions that we have investigated. We have constructed hybrid 2D correlation spectra from two series of time-dependent IR spectral variations observed for two kinds of reactions.

Theory

Synchronous and asynchronous spectra can be expressed by linear algebra.[15,17] In general, an experimental matrix **M** can be viewed as a product

$$\mathbf{M} = \mathbf{WS} \tag{1}$$

where **W** ($w \times n$) is a matrix of the n pure spectra (w points) and **S** ($n \times s$) is a matrix of the n concentration profiles (s points). Synchronous variable−variable ($\Phi_{vv}(\upsilon_1, \upsilon_2)$) and sample−sample ($\Phi_{ss}(s_1, s_2)$) 2D correlation spectra can be calculated by eqs 2A,B, respectively. (One must note that 2D correlation spectroscopy is not limited by the experimental matrix **M** of bilinear form (eq 1). It works even in the case where the experimental matrix is generated by nonlinearity.)

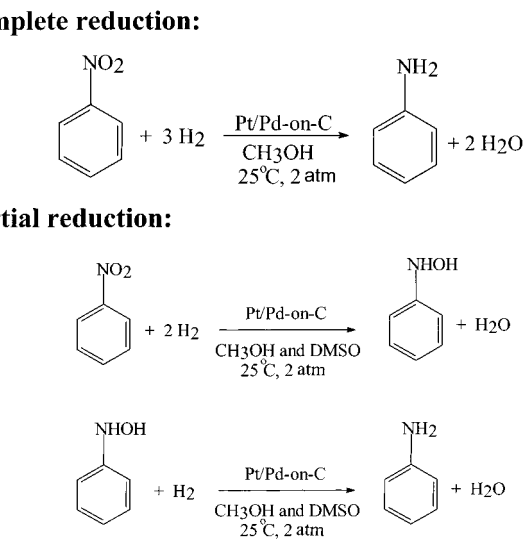

Figure 1. Reaction pathways of (A) complete reaction and (B) DMSO-modified reactions.

$$\Phi_{vv}(\upsilon_1, \upsilon_2) = 1/(s-1)\mathbf{MM}^{T} \tag{2A}$$

$$\Phi_{ss}(s_1, s_2) = 1/(w-1)\mathbf{M}^{T}\mathbf{M} \tag{2B}$$

where the matrix **M** represents dynamic spectra.[15,17] The corresponding asynchronous correlation spectra, $\Psi_{vv}(\upsilon_1, \upsilon_2)$ and $\Psi_{ss}(s_1, s_2)$ can be obtained by eqs 3A, B, respectively,

where **H** represents Noda's modification of the Hilbert transform matrix, called the Hilbert−Noda transform matrix.[5]

$$\Psi_{vv}(\upsilon_1, \upsilon_2) = 1/(s-1)\mathbf{MHM}^{T} \tag{3A}$$

$$\Psi_{ss}(s_1, s_2) = 1/(w-1)\mathbf{M}^{T}\mathbf{HM} \tag{3B}$$

Now let us consider hybrid 2D correlation spectra. Suppose the data obtained in two-perturbation (for example, time t and temperature T) dependent spectroscopic measurements are collected in a three-way array with the (i, j, k)th element denoting the spectral value at the ith time, the jth temperature, and the kth wavenumber (Figure 2).[25] Case I (A) is that a slice matrix in t order and another slice matrix in T order are taken to investigate the correlation between these two perturbations. Case II (B) is that two slice matrixes in T (or t) order are taken to investigate the correlation between these two perturbations. Case III (C) is that a slice matrix in t (or T) order and another slice matrix whose the ith column is the spectra obtained at the ith time and the jth temperature are taken to investigate the correlation between these two perturbations. Let us consider the three cases in more detail.

(I) *2D Correlation Spectra Calculated by Using Two Independent Spectral Data Sets Obtained under Two Kinds of Perturbations (Figure 2A).* As an example, one can use temperature−pressure hybrid 2D correlation spectroscopy. For this case, one can represent experimental data obtained under temperature ($\mathbf{M}_T$) and pressure ($\mathbf{M}_P$) perturbations as follows:

$$\mathbf{M}_1 = \mathbf{M}_T = \mathbf{WS}_T \tag{4A}$$

$$\mathbf{M}_2 = \mathbf{M}_P = \mathbf{WS}_P \tag{4B}$$

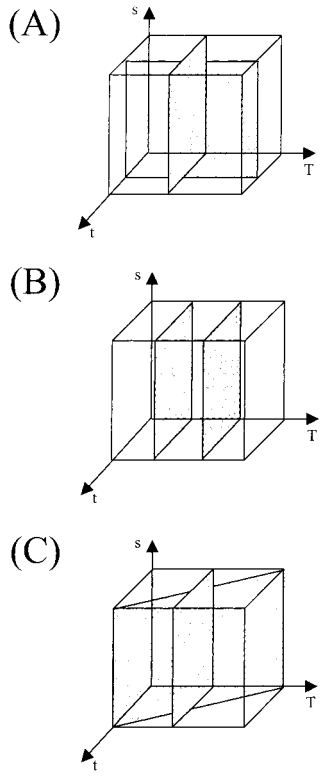

Figure 2. Physical illustration of three cases to construct hybrid 2D correlation spectra: (A) case I; (B) case II; (C) case III.

(II) *2D Correlation Spectra Constructed by Using One Spectral Data Set Obtained under Physically Coupled Perturbation or Related Perturbations (Figure 2B).* As an example, one can use hybrid 2D correlation spectroscopy of time- and temperature-dependent spectral changes. For this example, one can represent experimental data as follows:

$$\mathbf{M}_1 = \mathbf{M}_t = \mathbf{WS}_t \tag{5A}$$

$$\mathbf{M}_2 = \mathbf{M}_{t,T} = \mathbf{WS}_{t,T} \tag{5B}$$

(III) *2D Correlation Spectra Generated by Using Two Spectral Data Sets Obtained on the Basis of the Same Perturbation but underDifferent Conditions (Figure 2C).* As an example, one can use hybrid 2D correlation spectra of similar chemical reactions using different catalysts. For this case the experimental matrix can be represented as follows:

$$\mathbf{M}_1 = \mathbf{M}_{t1} = \mathbf{WS}_{t1} \tag{6A}$$

$$\mathbf{M}_2 = \mathbf{M}_{t2} = \mathbf{WS}_{t2} \tag{6B}$$

For all the three cases I−III, variable−variable and sample−sample 2D synchronous correlation spectra can be represent by the following equations respectively:

$$\Phi_{vv}(\upsilon_1, \upsilon_2) = 1/(s-1)\mathbf{M}_1\mathbf{M}_2^{\mathrm{T}} \tag{7A}$$

$$\Phi_{ss}(s_1, s_2) = 1/(w-1)\mathbf{M}_1^{\mathrm{T}}\mathbf{M}_2 \tag{7B}$$

or

$$\Phi_{vv}(\upsilon_1, \upsilon_2) = 1/(s-1)\mathbf{M}_2\mathbf{M}_1^{\mathrm{T}} \tag{8A}$$

$$\Phi_{ss}(s_1, s_2) = 1/(w-1)\mathbf{M}_2^{\mathrm{T}}\mathbf{M}_1 \tag{8B}$$

For eqs 7A and 8A, the multiplication of $\mathbf{M}_1$ and $\mathbf{M}_2$ is valid only when the sample number in each of the two experiments is the same. The multiplication is often allowed for the synchronous sample−sample correlation spectra, eqs 7B and 8B, since the spectral range measured for a system under different perturbations is always the same.

The corresponding, variable−variable and sample−sample 2D asynchronous correlation spectra can be computed by the following equations respectively:

$$\Psi_{vv}(\upsilon_1, \upsilon_2) = 1/(s-1)\mathbf{M}_1\mathbf{H}\mathbf{M}_2^{\mathrm{T}} \tag{9A}$$

$$\Psi_{ss}(s_1, s_2) = 1/(w-1)\mathbf{M}_1^{\mathrm{T}}\mathbf{H}\mathbf{M}_2 \tag{9B}$$

or

$$\Psi_{vv}(\upsilon_1, \upsilon_2) = 1/(s-1)\mathbf{M}_2\mathbf{H}\mathbf{M}_1^{\mathrm{T}} \tag{10A}$$

$$\Psi_{ss}(s_1, s_2) = 1/(w-1)\mathbf{M}_2^{\mathrm{T}}\mathbf{H}\mathbf{M}_1 \tag{10B}$$

It is important to note that eqs 7 and 8 give the same 2D maps but different slice spectra since they are transposes of each other, while eqs 9 and 10 yield exactly the inverse 2D maps since they are asymmetric to each other.

In the case of sample−sample correlation spectroscopy $\Phi_{ss}(s_1, s_2)$ and $\Psi_{ss}(s_1, s_2)$ can become, for example, $\Phi ss(T, P)$ and $\Psi ss(T, P)$ or $\Phi_{ss}(t, T)$ and $\Psi_{ss}(t, T)$, respectively, as to the first and the third cases. Thus, one may associate them with hetero sample−sample correlation spectroscopy. In hetero sample−sample correlation spectroscopy, 2D correlation spectra have, for example, temperature and pressure on the two axes, and one can compare effects of the two kinds of perturbations on one system.

As the hybrid 2D correlation spectra give covariance between two variables in two data matrixes, the autopeaks in the synchronous map indicate that the corresponding variables exhibit great variability. The appearance of cross-peaks in the synchronous map reveals that the associated two variables have correlated or in-phase variability. The sign of the cross-peaks in the synchronous map implies that these two variables vary in the same direction or in reverse directions. The cross-peaks in the asynchronous map suggest the out-of-phase variability between two variables. The sign of cross-peaks, coupled with the corresponding cross-peaks in the synchronous map, signifies the sequence of the variations of two variables.

Experimental Section

Chemical Reactions. Two kinds of catalytic hydrogenation reactions of nitrobenzene are investigated in this study. Hereafter, we call them system A and system B (Figure 1A,B). The details of experimental conditions (reactant, catalysts, solvents, etc.) for both reactions were reported elsewhere.[24] For system A, the complete hydrogenation, the solvent (water−methanol mixture), nitrobenzene, and mixed catalysts were charged into a reaction vessel and purged with nitrogen to eliminate headspace air that could cause deflagration/detonation hazards.[24] System B, the modified catalyst reaction, included the addition of dimethyl sulfoxide (DMSO) with the above mixture. Each hydrogenation was carried out isothermally at 298 K.

IR Spectral Measurements. All the spectra were measured with an ASI Applied Systems React-IR 1000 spectrometer connected to a 42 in. articulating transfer optics and optical sensing probe. The probe contained a zinc sulfide internal

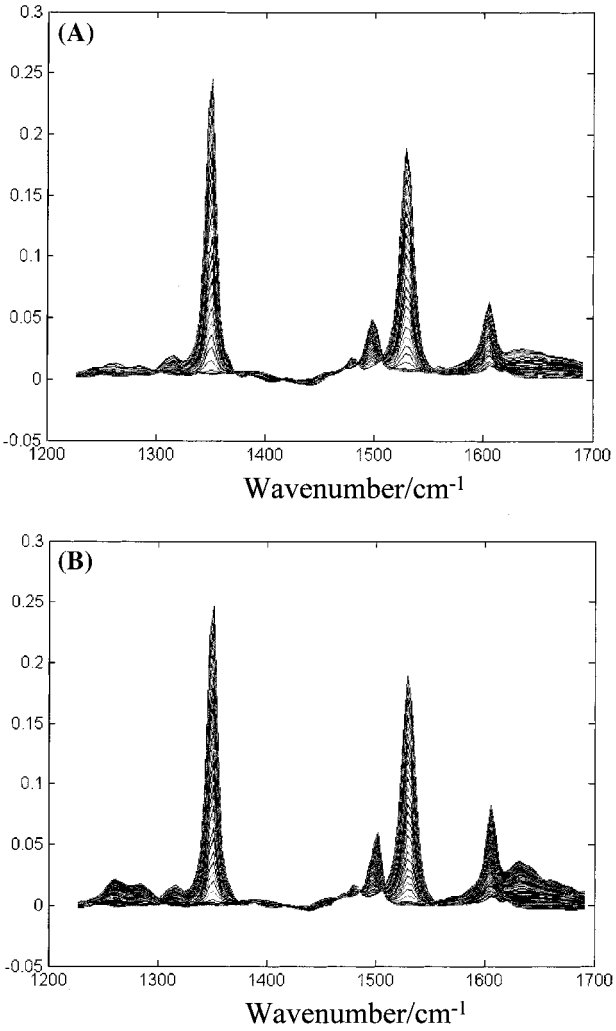

Figure 3. Time-dependent IR spectra in the range of 1800−1200 cm^{-1} measured during the hydrogenation of nitrobenzene: (A) complete reaction; (B) DMSO-modified reaction.

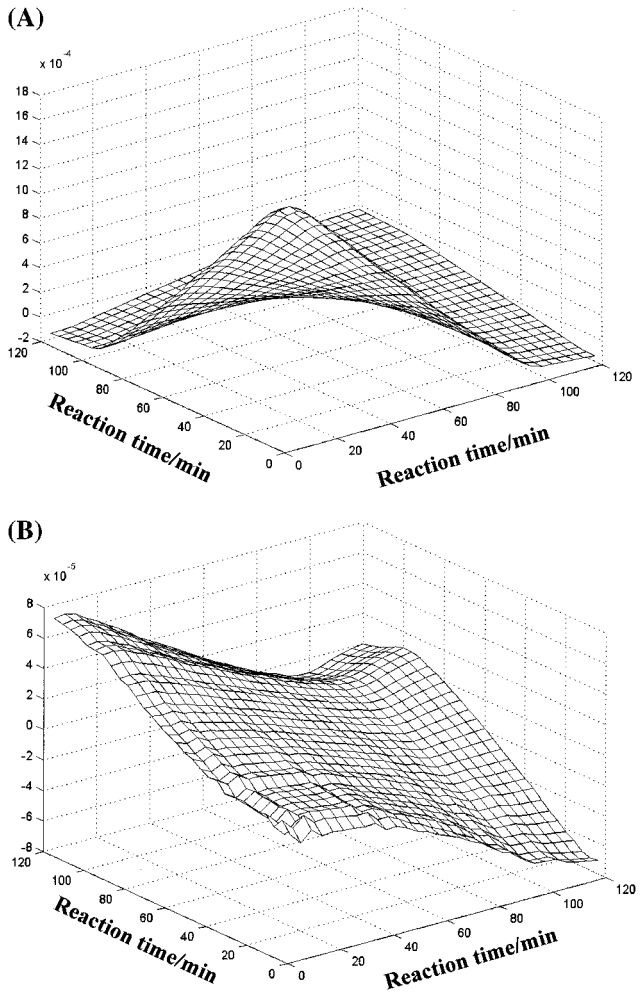

Figure 4. (A) Synchronous and (B) asynchronous sample−sample 2D correlation spectra calculated from the spectra shown in Figure 3A.

reflectance sensor. The analyzer used a deuterium triglyceride (DTGS) detector. Measurement of spectra took place automatically at 4 min intervals for the duration of the reaction. The spectra were obtained in the 1900−650 cm^{-1} region with a spectral resolution of 8 cm^{-1} by acquiring 256 coaveraged scans.

Data Pretreatment and Calculation of 2D Correlation Spectra. Synchronous and asynchronous correlation spectra were calculated using the algorithm developed by Noda.[2,26] Before the calculation of the matrixes was carried out, the mean centering of spectra was performed for the wavenumber−wavenumber correlation, while the mean centering of concentrations was performed for the sample−sample correlation.[15,16] Normalization was not carried out for this study. All the spectra were subtracted by the background spectra of the solvents prior to 2D correlation analysis.

Results and Discussion

1. Time-Dependent IR Spectra of the Two Kinds of Catalytic Hydrogenation Reactions. Figure 3A,B shows time-dependent IR spectra in the 1800−1200 cm^{-1} region of the complete (system A) and DMSO-modified (system B) hydrogenation reactions of nitrobenzene, respectively. Bands at 1529 and 1350 cm^{-1} that decrease with time are assigned to the NO_2 antisymmetric and symmetric stretching modes of nitrobenzene, respectively.[24] Three bands at 1606, 1500, and 1262 cm^{-1} that increase with time are due to $-NH_2$ deformation, ring stretching (ν_{19a}), and phenyl C−N stretching modes of aniline, respectively.[24] The spectra in Figure 3A,B look very similar to each other, but Kwasny et al.[24] found subtle but important spectral changes near 1500 cm^{-1} due to a reaction intermediate in the IR spectra of system B. The time-dependent intensity decreases in the bands at 1529 and 1350 cm^{-1} of the reactant and the concomitant intensity increases in the bands at 1606, 1500, and 1262 cm^{-1} of the product are consistent with the direct conversion of nitrobenzene to aniline in the reaction of system A. However, close inspection of the nitrobenzene and aniline bands in system B indicates that intensity variations of some bands occur out-of-phase.[24] Kwasny et al.[24] used an algorithm named OPUS1 resident in the IR monitoring software to analyze the spectra. OPUS1 is capable of postprocessing a reaction file to create relative concentration profiles and spectra of reaction mixture components. We apply the existing 2D and hybrid 2D correlation analyses to investigate the mechanism of the reactions of systems A and B.

2. Conventional Sample−Sample 2D Correlation Spectroscopy of the Two Kinds of Catalytic Hydrogenation Reactions. *System A: Complete Reaction.* Figure 4A,B shows sample−sample synchronous and asynchronous correlation spectra constructed from the time-dependent spectral variations in Figure 3A, respectively. In this case the sample−sample correlation spectroscopy is the time−time correlation spectroscopy. The strong positive values along the diagonal line in the synchronous spectrum indicate the strong correlation of the

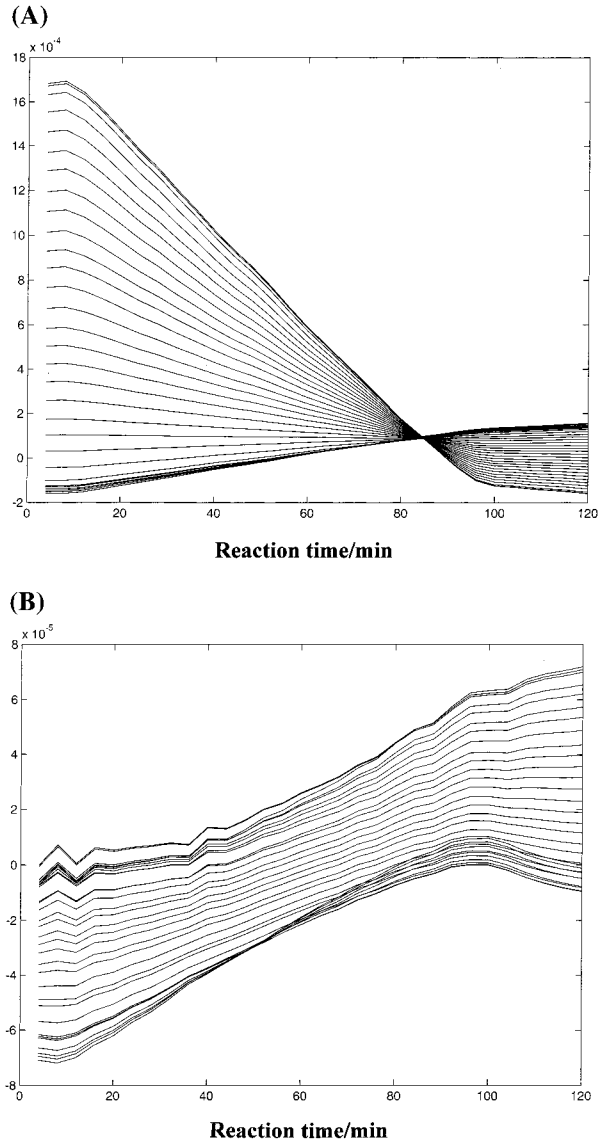

Figure 5. (A) Slice spectra obtained from Figure 4A. (B) Slice spectra obtained from Figure 4B.

reactant at the beginning of the reaction (Figure 4A). The synchronous spectrum clearly shows a marked decrease of the concentration of the reactant (nitrobenzene) and a slow increase of the product (aniline) at the same time up to no. 24 spectrum (corresponding to 96 min after the initiation of reaction), which corresponds to the end point of reaction. The dynamics of the reaction is revealed clearly by the sample−sample synchronous correlation map displayed in Figure 4A. The asynchronous spectrum gives very weak correlation (note the unit of *y* axis), suggesting slight nonproportionality in the rates of the concentration variations near the end point of reaction. The rate of the consumption of the reactant and that of the formation of the product are almost constant through the whole reaction process.

Slice spectra extracted from the synchronous and asynchronous spectra are exhibited in Figure 5A,B, respectively. The dynamics of complete reaction (system A) is shown more clearly in Figure 5A. The results in Figures 4 and 5 confirm the absence of any intermediate since its existence would alter the profile of the formation of the product relative to that of the consumption of the reactant.

System B: DMSO-Modified Hydrogenation Reaction. Figure 6A,B displays the sample−sample synchronous and asynchronous correlation spectra constructed from the series of spectra

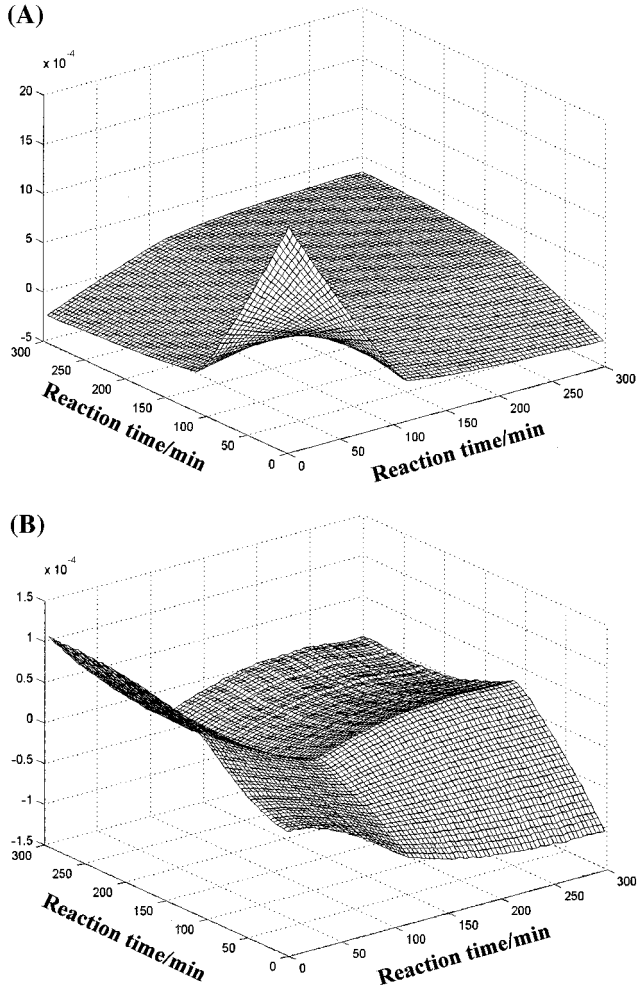

Figure 6. (A) Synchronous and (B) asynchronous sample−sample correlation spectra calculated from the spectra shown in Figure 3B.

in Figure 3B. Figure 7A,B gives the corresponding slice spectra. Note that significant differences are observed between the synchronous spectra shown in Figures 4A and 6A. The following differences are noted in the sample−sample synchronous spectra for systems A and B: (a) The correlation between the reactants is stronger in the synchronous spectrum of system B. (b) The positive correlation between the products is observed with a turn at the no. 24 spectrum (96 min) in system A. (c) The full consumption of nitrobenzene takes longer by about 20 min in system B up to the no. 29 spectrum (116 min), as revealed more clearly by the slice in Figure 7A. (d) The consumption of nitrobenzene and the formation of aniline do not occur in-phase in system B, which means that there is an intermediate in the modified reaction. (e) The formation of aniline takes place much more slowly in the modified reaction. The end point of reaction changes from 96 min for the complete reaction to over 4 h for the modified reaction.

It is noteworthy that though the conclusions c and e can also be obtained from the original spectra in Figure 3A,B by examining a few bands, the difficulty may arise in the interpretation of the reaction kinetics. This is due to the fact that the profiles of spectral changes at different bands show distinguished behavior in a system containing more than one reaction. Conclusions a−c cannot be drawn directly via inspecting the spectra in Figure 3A,B. In a sense, this demonstrates the potential of the sample−sample 2D correlation analysis.

The asynchronous spectrum in Figure 6B and its slice spectra in Figure 7B show a maximum positive correlation at (4, 300)

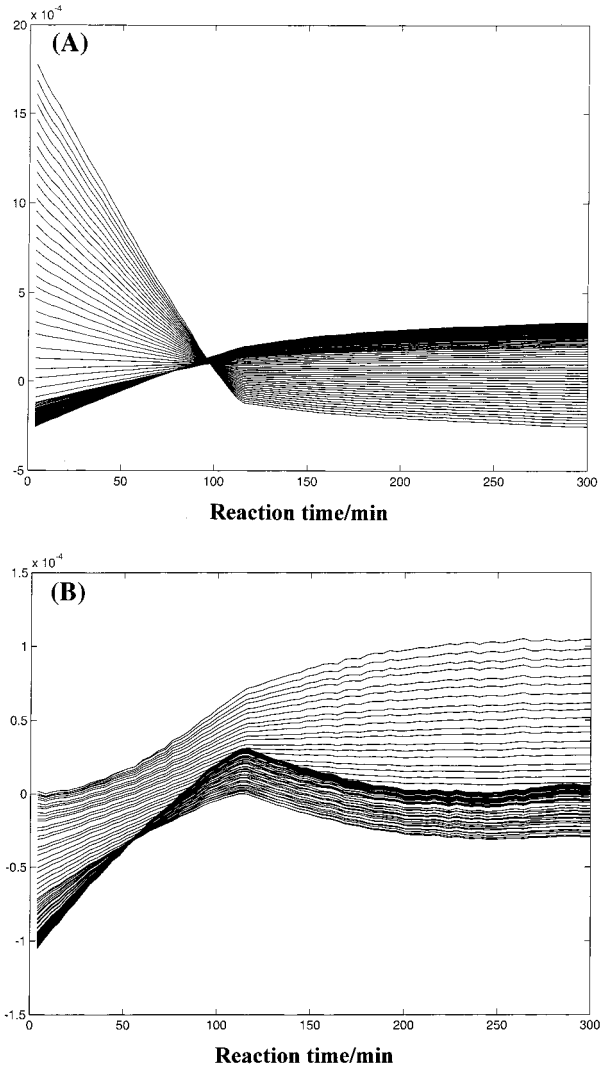

Figure 7. (A) Slice spectra obtained from Figure 6A. (B) Slice spectra obtained from Figure 6B.

and a minimum negative correlation at (300, 4), revealing the distinct nonproportionality in the rates of the concentration variations in these two points. An obvious change with a significant turn is observed at the no. 29 spectrum (116 min) (Figures 6B and 7B). These observations elucidate that the rate of reactant consumption and that of product formation are not uniform in the whole reaction range with the significant change at the no. 29 spectrum (116 min) and reach their maximum at (4, 300) or (300, 4). The significant turn in the asynchronous spectrum may correspond to the full consumption of nitrobenzene and the initiation of aniline formation in the reaction and, therefore, may also correspond to the maximum concentration of the intermediate. However, there is still no solid evidence to confirm the existence of an intermediate in the sample−sample correlation spectra.

3. Sample−Sample Hybrid 2D Correlation Spectroscopy between System A and System B. The purpose of generating the hybrid 2D correlation between systems A and B is to find the similarity and the differentiation in the dynamics between these two reactions. Since the end point of reaction in system A is located at the no. 24 spectrum (96 min) and the formation of aniline lasts until the no. 60 spectrum (240 min) in system B, we construct hybrid 2D correlation spectra by choosing the first 24 spectra from system A and the first 60 spectra from system B. Figure 8A,B shows the sample−sample synchronous

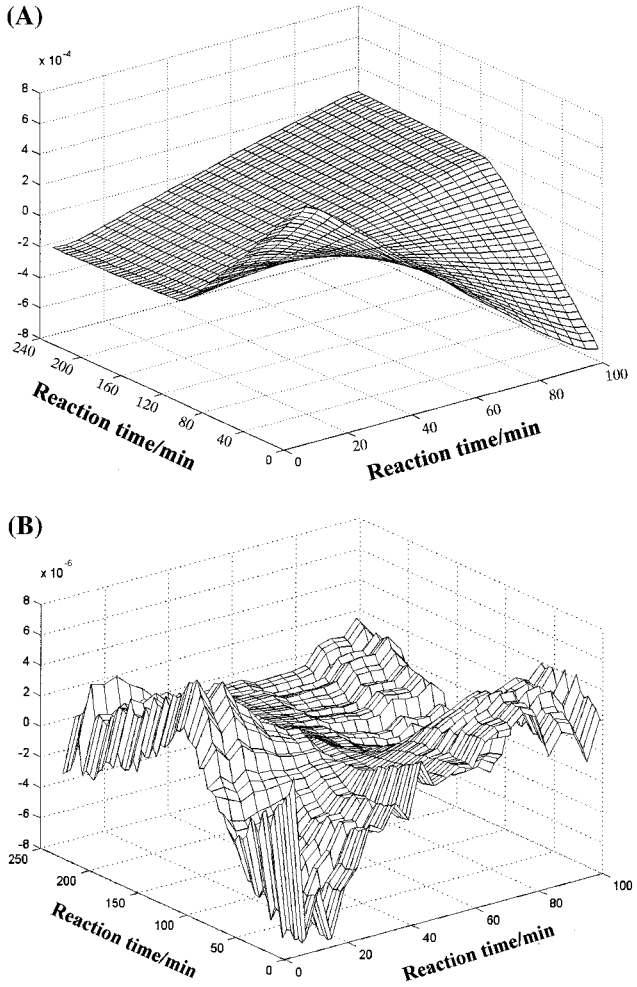

Figure 8. (A) Synchronous and (B) asynchronous sample−sample hybrid 2D correlation spectra constructed form the first 24 spectra in Figure 3A and the first 60 spectra in Figure 3B.

and asynchronous hybrid 2D correlation spectra constructed from them, respectively.

From the synchronous spectrum, one can see a maximum correlation of the reactant at (4, 4), which means the high correlation of the decreasing rate of nitrobenzene at the start point of both reactions. This maximum correlation value goes down along the two axes with different rates and reaches a minimum negative value at (96, 4) and a weak negative value at (4, 240). The difference in the rates along the two axes and that in the magnitudes at (96, 4) and (4, 240) reveal the differentiation of the kinetic vectors along the two axes. The strong negative value at (96, 4) elucidates high concentrations of completely different species, aniline at the no. 24 spectrum in system A and nitrobenzene at the no. 1 spectrum in system B. This supports the conclusion that there is no or very little aniline formation at the beginning of the reaction in system B while the formation of aniline starts from the initiation of the reaction in system A. A medium positive value at (96, 240) and a turn from negative to positive value at the no. 29 spectrum (116 min) in system B reveal that there is the correlation in the rate of aniline formation with a start from the no. 29 spectrum (116 min) in system B. Therefore, the hybrid 2D correlation in Figure 8A yields directly all the information that we have obtained separately from the two independent 2D correlation spectra in Figures 4A and 6A.

The hybrid 2D asynchronous spectrum in Figure 8B provides important information about the sequential or unsynchronized

variations. Note that there is a strong positive correlation at (96, 4) and at (96, 240). Another positive correlation is observed at (4, 116). A strong negative correlation is observed at (4, 240). Weak correlations around zero are observed between the no. 15 spectrum in system A and all the spectra in system B.

Usually, a strong correlation is observed between two groups of samples that have the highest values at the samples with the highest concentrations of the species.[15] For a simple two-component system with nonequal uniform concentration changes a reactant and a product show a correlation function whose maximum points are located at positions of the highest concentration at the start and end points of the reaction as revealed in Figures 4B and 6B. However, an obvious positive correlation is also observed at (4, 116) in the hybrid asynchronous spectrum in Figure 8B, which may reveal the highest concentration of the intermediate at the no. 29 spectrum (116 min) in system B. This result cannot be achieved by the normal sample−sample correlation analyses in Figures 4 and 6. To confirm that the turn at the no 29 spectrum is due to the intermediate or to the full consumption point of the reactant, we construct wavenumber−wavenumber hybrid 2D correlation spectra that supply complementary information about the mechanism of the reaction.

4. Wavenumber−Wavenumber Hybrid 2D Correlation Spectroscopy between System A and System B. The existence of an intermediate in system B is suggested by sample−sample hybrid 2D correlation spectroscopy. However, the spectral features of the intermediate need to be investigated more extensively. We, of course, know what the intermediate is (Figure 1). The intermediate has a structure very similar to that of aniline and should show bands near 1606, 1500, and 1286 cm^{-1}. It is not easy to distinguish the spectrum of the intermediate from that of aniline.[24] To identify the bands due to the intermediate, deconvolution of the bands arising from the intermediate and final product must be performed. Therefore, hybrid 2D wavenumber−wavenumber correlation analysis has been applied. The spectral region of 1465−1510 cm^{-1} has been selected because aniline has a strong band around 1500 cm^{-1} due to the ν_{19} mode.[24] To keep the numbering consistent with the spectra in system A and to reveal bands arising from phenylhydroxylamine, the intermediate, clearly, we have selected the nos. 1−24 spectra from system A and two spectral groups, nos. 1−24 and nos. 30−53, from system B to construct the wavenumber−wavenumber hybrid 2D correlation spectra. Figure 9A,B shows hybrid 2D wavenumber−wavenumber synchronous and asynchronous spectra generated from the nos. 1−24 spectra of system A and nos. 1−24 spectra of system B, respectively. The corresponding hybrid 2D spectra generated from the nos. 1−24 spectra of system A and nos. 30−53 spectra of system B are shown in Figure 10A,B, respectively.

In Figure 9A two bands can be identified at 1502 and 1483 cm^{-1} along the *x* axis (system A). The band at 1502 cm^{-1} is assigned to a ring stretching mode (ν_{19a}) of aniline.[24] Along the *z* axis (system B) two bands can be observed at 1498 and 1479 cm^{-1}. The band at 1498 cm^{-1} is assigned to a ring stretching mode (ν_{19a}) of phenylhydroxylamine.[24] Its appearance confirms the existence of intermediate at the first stage of the reaction in system B. A positive cross-peak at (1502, 1498) cm^{-1} reveals that the intensities of both bands increase in-phase, although they arise from the two different systems. This result also reveals that the concentration of phenylhydroxylamine increases up to the no. 29 spectrum of system B. This is consistent with the conclusion that we have reached from the sample−sample hybrid 2D correlation; that is, the highest concentration of phenylhydroxylamine occurs at the no. 29 spectrum of system B.

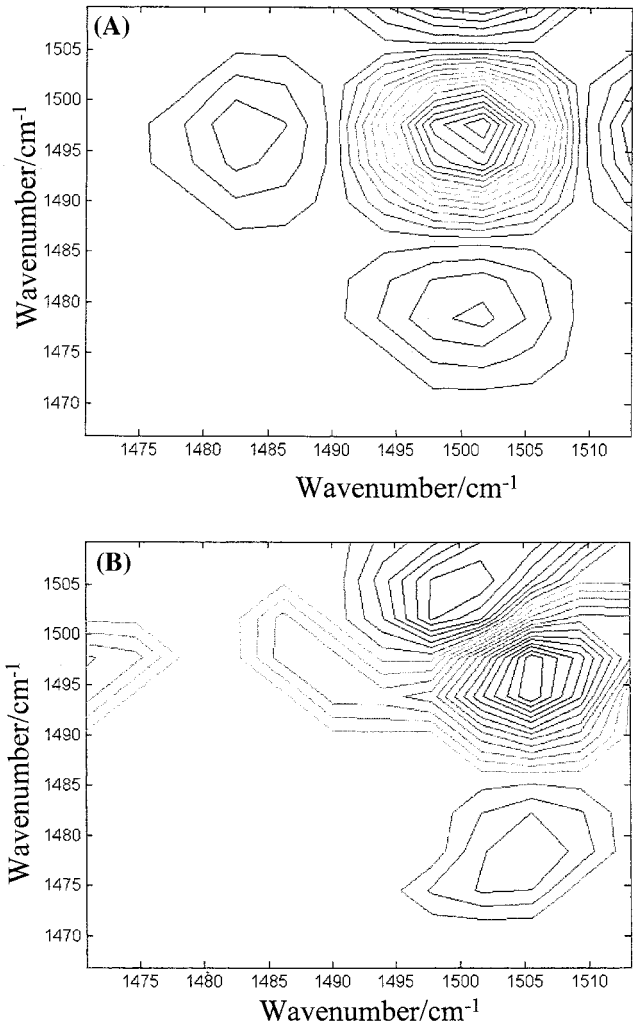

Figure 9. (A) Synchronous and (B) asynchronous wavenumber−wavenumber hybrid 2D correlation spectra in the range of 1465−1515 cm^{-1} constructed from the first 24 spectra in Figure 3A and the first 24 spectra in Figure 3B.

The asynchronous spectrum in Figure 9B shows that the band at 1502 cm^{-1} splits into two bands at 1506 and 1502 cm^{-1}, and the band at 1498 cm^{-1} along the *z* axis splits into two bands at 1498 and 1494 cm^{-1}. A new band at 1506 cm^{-1} along the *z* axis indicates the appearance of aniline in the first stage of the reaction. It cannot be detected in the synchronous hybrid 2D correlation spectrum because of the strong overlap of the band at 1498 cm^{-1}. This result reveals that the formation of aniline is initiated at the first stage of system B. However, it forms very slowly in that period.

The hybrid 2D correlation spectra in Figure 10A,B provide complementary information about the reaction dynamics both in systems A and B. The synchronous spectrum in Figure 10A yields clear evidence for the two bands at 1494 and 1501 cm^{-1} along the *z* axis. These two bands are assigned to ring vibrational modes of phenylhydroxylamine and aniline, respectively.[24] Cross-peaks at (1502, 1494) and (1502, 1501) cm^{-1} reveal that the intensity changes at 1502, 1501, and 1494 cm^{-1} take place synchronously. The signs of the cross-peaks at (1502, 1494) and (1502, 1501) cm^{-1}, negative and positive, illustrate the opposite and same directions of band intensity changes at 1494 and 1501 cm^{-1} in system B and at 1502 cm^{-1} in system A,

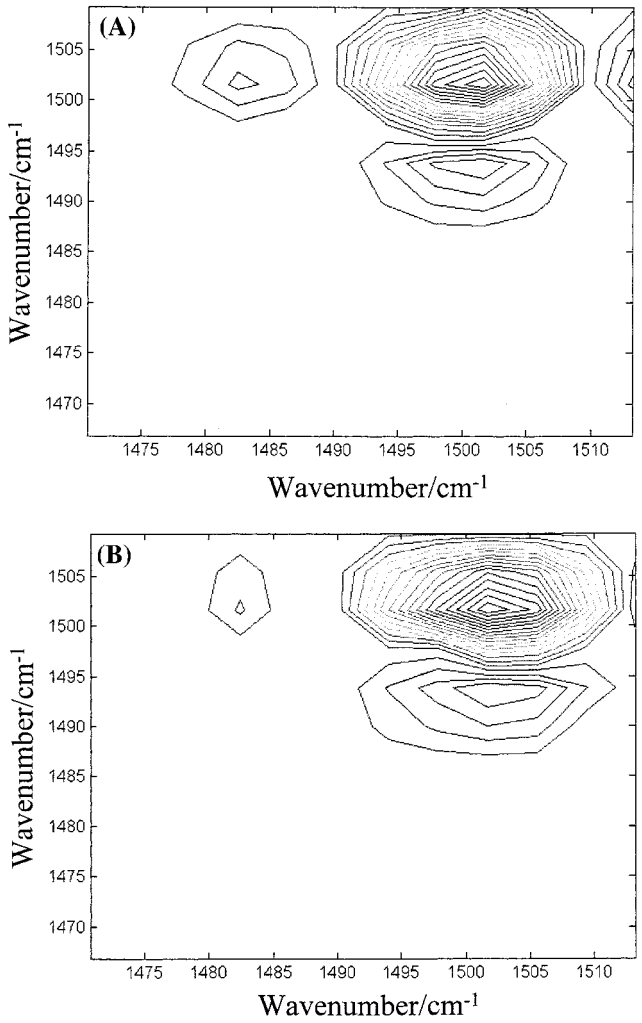

Figure 10. (A) Synchronous and (B) asynchronous wavenumber−wavenumber hybrid 2D correlation spectra in the range of 1465−1515 cm^{-1} constructed from the first 24 spectra in Figure 3A and spectra nos. 30−53 in Figure 3B.

respectively. This means that in the second stage in system B the conversion of phenylhydroxylamine to aniline occurs with time.

Conclusions

We have opened a new possibility of the generalized 2D spectroscopy in this study. Hybrid 2D correlation spectroscopy enables one to explore directly the correlations between two systems or spectral data sets obtained under two different perturbations. As in the case of conventional 2D correlation spectroscopy, the hybrid 2D correlation spectroscopy has also variable−variable and sample−sample correlation spectroscopy. This new type of 2D correlation has been applied to time-dependent IR spectra of two kinds of the catalytic hydrogenation reactions of nitrobenzene. The following conclusions can be reached from the sample−sample and wavenumber−wavenumber hybrid 2D correlation spectroscopy: (1) Reaction mechanisms of two different kinds of reactions can be explored more clearly and directly by hybrid 2D correlation analysis. It has been found that the concentration of the intermediate reaches the maximum at the no. 29 spectrum (96 min) of system B and that the formation of aniline is initiated at the first stage of system B. (2) Fine spectral differences between the product, aniline, and the intermediate, hydroxylamine, can be distinguished directly by wavenumber−wavenumber hybrid 2D correlation analysis, which confirms the existence of the intermediate in the DMSO-modified partial reduction.

Acknowledgment. The authors thank Dr. R. S. Kwasny, Dr. R. A. Giusto, and Dr. N. E. Van Order, Jr., of ASI, Applied Systems (Millersville, MD), for their generous offer of the spectral data and Dr. S. Ochiai of ST Japan Co. (Tokyo, Japan) for the introduction of the spectral data for the application of hybrid 2D correlation spectroscopy. The authors also thank Dr. Šašić of our laboratory for valuable discussion about sample−sample correlation spectroscopy. This study was supported by a Grant-in-Aid to Y. Ozaki (11640516) from the Ministry of Education, Science, and Culture of Japan.

References and Notes

(1) Noda, I. *Appl. Spectrosc.* **1990**, *44*, 550.
(2) Noda, I. *Appl. Spectrosc.* **1993**, *47*, 1329.
(3) Ozaki, Y.; Noda, I. *Two-dimensional Correlation Spectroscopy*; American Institute of Physics: Melville, NY, 2000.
(4) Special focus issue: *Two-Dimensional Correlation Spectroscopy*. *Appl. Spectrosc.* **2000**, *54* (July).
(5) Noda, I.; Dowrey, A. E.; Marcott, C.; Story, G. M.; Ozaki, Y. *Appl. Spectrosc.* **2000**, *54*, 236A.
(6) Schultz, C. P.; Fabian, H.; Mantsch, H. H. *Biospectroscopy* **1998**, *4*, 19.
(7) Sefara, N. L.; Magtoto, N. P.; Richardson, H. H. *Appl. Spectrosc.* **1997**, *51*, 536.
(8) Wang, Y.; Murayama, K.; Myojo, Y.; Tsenkova, R.; Hayashi, N.; Ozaki, Y. *J. Phys. Chem. B* **1998**, *102*, 6655.
(9) Wu, Y.; Czarnik-Matusewicz, B.; Murayama, K.; Ozaki, Y. *J. Phys. Chem. B* **2000**, *104*, 5840.
(10) Nabet, A.; Pezolét, M. *Appl. Spectrosc.* **1997**, *51*, 466.
(11) Ren, Y.; Shimoyama, N.; Matsukawa, K.; Inoue, H.; Noda, I.; Ozaki, Y. *J. Phys. Chem. B* **1999**, *103*, 6475.
(12) Noda. I.; Liu, Y.; Ozaki, Y. *J. Phys. Chem.* **1996**, *100*, 8674.
(13) Jung, Y.-M.; Czarnik-Matusewicz, B.; Ozaki, Y. *J. Phys. Chem. B* **2000**, *104*, 7812.
(14) Czarnecki, M. A.; Wu, P.; Siesler, H. W. *Chem. Phys. Lett*. **1998**, *283*, 326.
(15) Šašić, S.; Muszynski, A.; Ozaki, Y. *J. Phys. Chem. A* **2000**, *104*, 6380.
(16) Šašić, S.; Muszynski, A.; Ozaki, Y. *J. Phys. Chem. A* **2000**, *104*, 6388.
(17) Šašić, S.; Muszynski, A.; Ozaki, Y. *Appl. Spectrosc.* **2001**, *55*, 343.
(18) Šašić, S.; Ozaki, Y. *Anal. Chem*. **2001**, *73*, 2294.
(19) Barton, W. F., II; Himmelsbach, D. E.; Duckworth, J. H.; Smith, M. J. *Appl. Spectrosc.* **1992**, *46*, 420.
(20) Czarnik-Matusewicz, B.; Murayama, K.; Wu, Y.; Ozaki, Y. *J. Phys. Chem. B* **2000**, *104*, 7803.
(21) Torrent, J.; Connelly, J. P.; Coll, M. G.; Ribó, M.; Lange, R.; Vilanova, M. *Biochemistry* **1999**, *38*, 159525.
(22) Panick, G.; Winter, R. *Biochemistry* **2000**, *39*, 1862.
(23) Noda, I, Doctoral Thesis, University of Tokyo, 1996; p 263.
(24) Kwasny, R. S.; Giusto, R. A.; Van Order, N. E., Jr. Proceedings of ASI Applied Systems 3rd Annual User's Forum, 1996.
(25) Sanchez, E.; Kowalski, B. R. *J. Chemom.* **1990**, *4*, 29.
(26) Noda, I. *Appl. Spectrosc.* **2000**, *54*, 994.